ADVANCED FUNCTIONAL MATERIALS

Supporting Information

Plasmon-Enhanced Photodetection in Ferromagnet/ Nonmagnet Spin Thermoelectric Structures

Chul-Yeon Jeon, Kwang Min Baek, Shinho Kim, Dong-Jun Kim, Min Seok Jang, Yeon Sik Jung, and Byong-Guk Park*

Supporting Information

Plasmon-enhanced Photodetection in Ferromagnet/Non-magnet Spin Thermoelectric Structures

Chul-Yeon Jeon, Kwang Min Baek, Shin Ho Kim, Dong-Jun Kim, Min Seok Jang, Yeon Sik Jung, and Byong-Guk Park

Table of contents

1. Thermoelectric voltage from CoFeB/W with Au nanorods

We performed additional measurements for a CoFeB/W bilayer using identical measurement conditions for the CoFeB/Pt bilayer shown in the Figure 2a in the main text. SI Figure 1 shows that spin thermoelectric voltage (ΔV) of the CoFeB/W samples with and without Au nanorods as a function of magnetic field along the x-direction (H_x). By introducing Au nanorods on top of the CoFeB/W, ΔV is enhanced by 45±6% compared to the reference sample without Au nanorods. This result confirms that the signal enhancement by the plasmon resonance of Au nanorods is generally observed in a ferromagnet/non-magnet bilayer system.
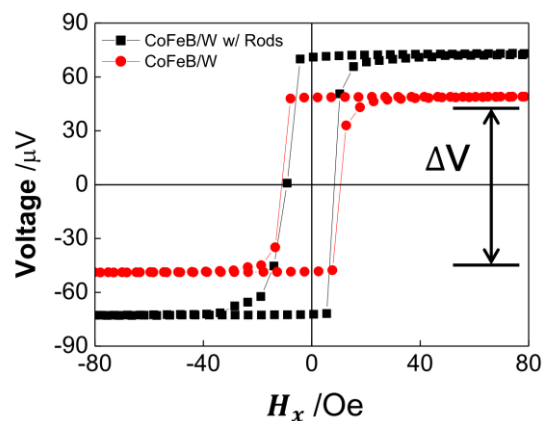
SI Figure 1 | Thermoelectric voltage versus magnetic field along the x-direction (H_x) for the CoFeB/W sample with (black) and without (red) Au nanorods. ΔV is defined as $V(H=80$ Oe)-$V(H=-80$ Oe). Here, the laser wavelength is 660 nm.

2. FDTD and COMSOL simulations

We estimated the temperature profile induced by laser illumination in the sample of Si (200 μm)/SiO$_2$ (200 nm)/CoFeB (8 nm)/Pt (3 nm)/MgO (1 nm)/Ta (1.5 nm)/ SiO$_2$ (50 nm)/Au (21 nm) nanorods by utilizing finite-difference time-domain (FDTD) simulation (Lumerical Inc.) and finite element method simulation (COMSOL Multiphysics), which is shown in Figure 5a of the main text. The material parameters of each layer for the simulations are listed in Table S1.

The FDTD simulation was employed to calculate the heat energy density generated within the structure. While an inclined monochromatic 660-nm Gaussian laser beam was used in the experiment, we adopted a plane wave as a source in the simulation to avoid cumbersome calculation. As the beam spot size (~5 μm) is much larger than the width (~30 nm) and pitch (~20 nm) of Au nanorods array, it is reasonable to assume that local optical response of Au nanorods is more or less same either from Gaussian wave or plane wave. So, both calculations were performed in a periodic cell illuminated by an inclined 660 nm plane wave where the magnitude of the electric field was set as the center value of Gaussian beam of a power of 60 mW and a beam spot size of 5 μm. As for the heat energy density, the distribution was later converted to Gaussian shape function to adequately reflect the actual experimental condition of the beam.

SI Figure 2 shows the result of the electromagnetic field ($|E|$) profile for the two polarization incidences, which are transverse and longitudinal to the Au nanorods. As shown in the transverse polarization, strong electromagnetic fields are generated between the rods and in the vicinity of the rod/air and rod/SiO$_2$ interface, indicating the localized surface plasmon resonance, while the enhancement of electromagnetic fields do not appear under longitudinal polarization. Furthermore, the result also shows that the intensity of the electromagnetic field profile between Au nanorods and bottom Si substrate is different for the two polarizations where it is found to be larger at the transverse polarization. We believe that

it is due to plasmonic light trapping from which light can be trapped between the plasmonic nanostructure and bottom reflector.[S1-S3] This is consistent with the results in Figure 4b and Figure 5b of the main text in which the reflectance (light absorption) shows the minimum (maximum) at the transverse resonance condition.

The calculated heat energy density profile from the light absorption was employed as a heat source for the COMSOL heat transfer simulation. The distribution of heat energy density was calculated based on Joule equation which is defined as, $P = \frac{\omega}{2}\text{Im}(\epsilon)|\mathbf{E}|^2 = \omega nk|\mathbf{E}|^2$, where, $\omega, \epsilon, n,$ and k are the angular frequency of laser, the material permittivity, the real and imaginary part of refractive index, respectively.

To eliminate numerical artifacts, the simulated cell was set as sufficiently large volume of $200{\times}200{\times}200$ μm^3, which includes air, Au nanorods, SiO_2, CoFeB/Pt and Si/SiO_2 substrate. The boundary temperature of the cell edges was set to be room temperature. The heat density distribution was then converted to Gaussian shape function, which is defined as, $Q(x,y,z) = P_{cell}(x,y,z)P_{period}(x,y)e^{-2(x^2+y^2)/w_0^2}$. Here, P_{cell}, P_{period}, and w_0 are the heat density distribution within a cell, the conversion function that converts P_{cell} to periodic function, and the half of beam spot size, respectively. The z-direction temperature profile shown in Figure 5c of the main text was calculated by averaging the temperatures within the area of 5×5 μm^2 on x-y plane from the center of Gaussian beam spot. To precisely describe temperature gradient of the CoFeB/Pt bilayers, the mesh size in the z direction is set to be 0.5 nm. As shown in the SI Figure 3, we found that the simulated cell size or the air convection does not alters the calculated result of temperature profile.

3. Device design for uniform illumination

With the sample geometry in the main text, the uniform illumination would induce a smaller temperature gradient in CoFeB/Pt bilayers than the focused illumination. We modify the sample geometry, which consists of a rectangular CoFeB/Pt film of a high aspect ratio (2 μm×200 μm) and Au nanorods of 2 μm×2 μm patterned only at the central region (SI Figure 4a). In such structure, the preferential absorption by the plasmonic structure could offer the thermal concentration of the area covered by Au nanorods.[S4] We simulated the vertical temperature gradient in the CoFeB/Pt layer under the laser illumination of 7 μm in diameter. The temperature difference along the CoFeB/Pt layer within the Au rod pattern is ~0.4 K, while that is ~0.2 K of the CoFeB/Pt without the Au rod (SI Figure 4b). Note that the simulated value under semi-uniform illumination is comparable to that induced by focused illumination. This demonstrates that a proper design of the sample with plasmonic nano-structures would have enough temperature gradient to achieve sizable thermoelectric voltage.

In addition, we would like to point out that the formation of thermopiles is an alternative way to detect the light signal in a large area.[S5] As the voltage signal can scale with the number of wire elements (SI Figure 4c), the thermopile with plasmonic structures allows our device to operate in a large area illumination.

Table S1 | Material parameters for the numerical calculations of heat energy density and temperature gradient. n : the real part of refractive index, k : the imaginary part of refractive index, C_p : heat capacity, ρ: density, κ : thermal conductivity.[S6-S10]

Parameter	Au	SiO$_2$	Si	Ta	MgO	Pt	CoFeB
n	0.164	1.46	3.837	1.52	1.733	2.39	2.567
k	3.24	0	0.016	2.28	0	4.28	3.51
C_p [J·kg^{-1}·K^{-1}]	128	1052	700	140	877	133	440
ρ [kg·m^{-3}]	19,300	2200	2330	16,650	3600	21,090	8220
κ [W·m^{-1}·K^{-1}]	320	1.4	150	57	42	72	10.3
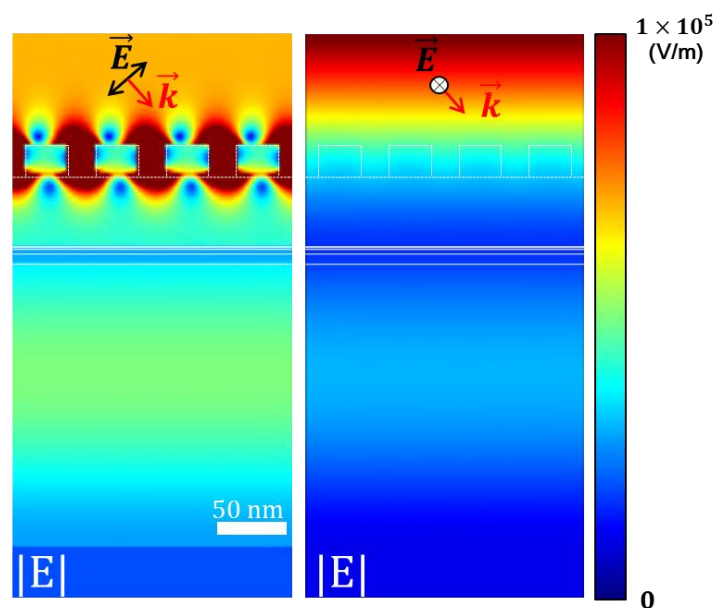
SI Figure 2 | FDTD results of electromagnetic field ($|E|$) profile from the polarized incidence that is transverse to rods (left) and longitudinal to rods (right), respectively. $\vec{E}$ denotes the electric field of incident light and $\vec{k}$ represents the wave vector where the incident angle is identical to the experimental condition. Color scale represents the magnitude (V/m) of the electric field.
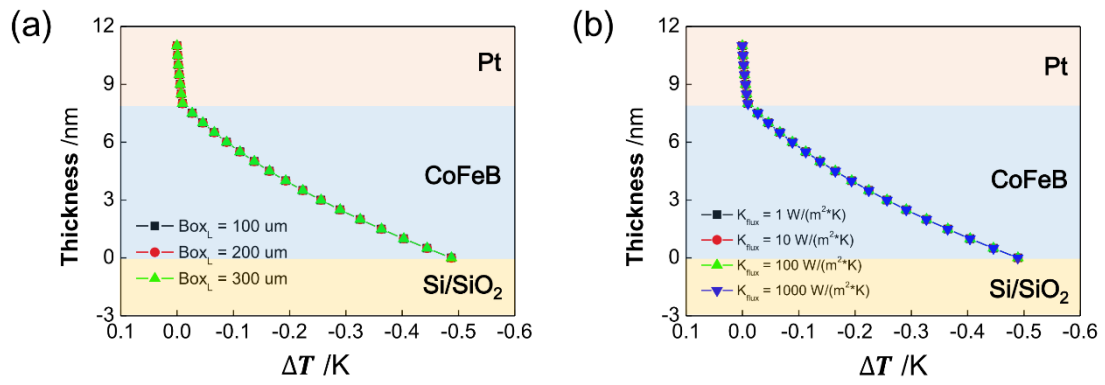
SI Figure 3 | (a) Effect of simulated cell size in temperature profile. (b) Temperature profile from the air convection.
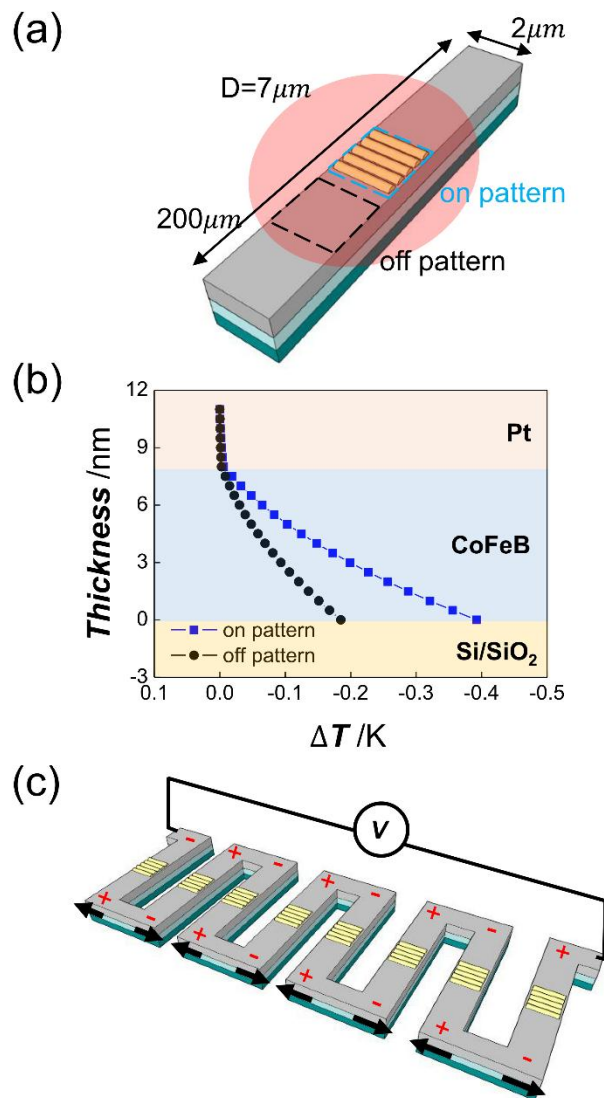
SI Figure 4 | (a) Schematic of a sample consisting of a rectangular CoFeB/Pt film of a high aspect ratio (2 µm × 200 µm) and Au nanorods of 2 µm × 2 µm patterned only at the central region. The red circle represents the laser diameter of 7µm. (b) Calculated temperature profile in the CoFeB/Pt layer for the area on pattern (blue) and off pattern (black), which is indicated as dashed squares. (c) Proposed device schematic for plasmon layer-coated spin thermopiles. The black arrows indicate the magnetization direction of the element wire, which can be controlled using an antiferromagnetic layer.

References

[S1]   Y. A. Akimov, W. S. Koh, *Plasmonics* **2011,** *6*, 155.

[S2]   V. E. Ferry, M. A. Verschuuren, H. B. Li, E. Verhagen, R. J. Walters, R. E. Schropp, H. A. Atwater, A. Polman, *Opt. Express* **2010,** *18*, A237.

[S3]   H. Tan, R. Santbergen, A. H. Smets, M. Zeman, *Nano Lett.* **2012,** *12*, 4070.

[S4]   K. W. Mauser, S. Kim, S. Mitrovic, D. Fleischman, R. Pala, K. Schwab, H. A. Atwater, *Nat. Nanotechnol.* **2017**, *12*, 770.

[S5]   D.-J. Kim, K.-D. Lee, S. Surabhi, S.-G. Yoon, J.-R. Jeong, B.-G. Park, *Adv. Funct. M ater.* **2016**, *26*, 5507-5514.

[S6]   A. Boehnke, M. Walter, N. Roschewsky, T. Eggebrecht, V. Drewello, K. Rott, M. Münzenberg, A. Thomas, G. Reiss, *Rev. Sci. Instrum.* **2013,** *84*, 063905.

[S7]   K.-D. Lee, D.-J. Kim, H. Y. Lee, S.-H. Kim, J.-H. Lee, K.-M. Lee, J.-R. Jeong, K.-S. Lee, H.-S. Song, J.-W. Sohn, S.-C. Shin, B.-G. Park, *Sci. Rep.* **2015,** *5*, 10249.

[S8]   D.-J. Kim, K.-D. Lee, S. Surabhi, S.-G. Yoon, J.-R. Jeong, B.-G. Park, *Adv. Funct. Mater.* **2016,** *26*, 5507.

[S9]   X. Liang, X. Xu, R. Zheng, Z. A. Lum, J. Qiu, *Appl. Opt.* **2015,** *54*, 1557.

[S10]   Material parameters, http://refractiveindex.info and http://www.webelements.com (accessed: November 2017).